

A new water-soluble Rh(III)-salophen complex as efficient catalyst for alcohol oxidation in aqueous medium

Biplab Banik^{a,b}, Podma Pollav Sarmah^a, Abhijit Dutta^c, Paritosh Mondal^c & Pankaj Das^{a,*}

^aDepartment of Chemistry, Dibrugarh University, Dibrugarh 786 004, Assam, India

^bDepartment of Chemistry, Tinsukia College, Tinsukia 786 125, Assam, India

^cDepartment of Chemistry, Assam University, Silchar 788 011, Assam, India

Email: pankajdas@dibru.ac.in

Received 21 June 2018; revised and accepted 18 December 2018

A new water soluble rhodium(III) complex $[\text{Rh}(\eta^4\text{-L})\text{Cl}]$ (**1a**) has been isolated from the reaction between $\text{RhCl}_3 \cdot 3\text{H}_2\text{O}$ and salophen ligand [**L** = N,N'-bis(salicylidene)-1,2-phenylenediamine (**a**)] in 1:1 molar ratio in dichloromethane solution. The complex **1a** has been characterized by FT-IR, UV-vis, ESI-MS, ^1H and ^{13}C NMR spectroscopy. Theoretical calculations (B3LYP) and spectroscopic evidence recommends that the ligand **a** coordinates to the Rh centre through imine N and phenolic O donor atoms. The complex **1a** emerged out to be an effective catalyst for oxidation of alcohols in water. Excellent yields of carbonyl compounds have been acquired for a comprehensive assortment of substrates with H_2O_2 as oxidant at a relatively low loading of catalyst. Thus, the Rh(III)- H_2O - H_2O_2 catalytic system could act as an environmentally benign alternative to oxidation methods in conventional organic solvents.

Keywords: Rhodium(III) complexes, Salophen, Water soluble, Density functional theory calculations, Aqueous catalysis

The transition metal catalyzed selective oxidation of alcohols to aldehydes or ketones without traceable over-oxidation products is one of the most considerable functional group transformations in synthetic organic chemistry for construction of a diverse range of intermediates in pharmaceutical industries¹⁻¹⁰. Conventional oxidation methods involve stoichiometric inorganic oxidants such as hexavalent chromium and heptavalent manganese, which are very atom inefficient and generate copious amounts of hazardous inorganic waste¹¹⁻¹³. With escalating environmental concerns, over the years, much attention has been paid to catalytic oxidation reactions in the presence of environmentally green oxidants^{5-8,14-16}. Among the preferred oxidants, hydrogen peroxide has proved to be a very promising oxidant for both laboratory and industrial production because of its low cost, atom efficiency, higher content of active oxygen and environmentally benign properties. Particularly, in aqueous solution, H_2O_2 is greatly attractive due to release of active oxidative species and the production of water as the sole by-product. In the last few years, water has gained notable attention as an environmentally harmless and economically preferable alternative solvent for organic reactions including alcohol oxidation

reactions due to its high accessibility, non-flammability and mild behaviour. However, in majority of the cases, organic reactions in aqueous media remained ineffective mainly due to insolubility of the metal complex in water. However, there exist a few examples^{9,17-21} where alcohol oxidation could be accomplished in aqueous condition, but such systems generally needed high catalyst loading¹⁷, high temperature¹⁸, biphasic solvent system¹⁹, use of additives²⁰, high concentration of base²¹ etc. Thus, there is sufficient opportunity for the development of efficient catalytic systems that can promote alcohol oxidation reactions in aqueous system with low metal loading under mild reaction conditions.

It is well recognized that in transition metal-based catalysis, the activity and selectivity of a catalytic system can be controlled by the inherent feature of the ligand anchored to the metal, and thus selecting a suitable ligand is pivotal for the catalyst's performance. Among different N-based ligands, the multidentate Schiff bases have acquired noteworthy attention, primarily because of their simple synthetic methodology and higher stability²²⁻²³. Furthermore, the most fascinating characteristic of Schiff base ligands is that their stereo-electronic properties can be easily fine tuned by suitably selecting the condensing

partners and they can stabilize metal ions in diverse oxidation states²⁴. Literature study reveals that these multidentate Schiff base ligands have successfully been used as catalysts for different reactions like oxidation²⁵⁻³⁰, polymerization³¹, hydrogenation³², reduction³³, epoxidation³⁴⁻³⁵, and cross-coupling reactions³⁶⁻³⁸.

Hence, as a part of our ongoing work on Schiff base derived catalytic system³⁹⁻⁴² we report herein the synthesis of a new water-soluble rhodium(III) complex containing N₂O₂-type Schiff base ligand. Its activity as alcohol oxidation catalyst in aqueous media has been explored.

Materials and Methods

The RhCl₃.3H₂O, salicylaldehyde, and *o*-phenylenediamine were procured from Sigma-Aldrich. The various substrates for alcohol oxidation and other general chemicals were purchased from various firms like Sigma-Aldrich, Merck, Spectrochem and Rankem. The solvents of analytical grade were procured from Spectrochem and distilled prior to use. The elemental (CHN) analyses were carried out using Perkin Elmer 2400 series II analyser. Mass spectrum of the complex was recorded on a Waters ZQ-4000 ESI/MS. The IR spectra (4000–400 cm⁻¹) were recorded in KBr pellet by using Shimadzu (Prestige-21) spectrophotometer. The ¹H and ¹³C NMR spectra were recorded on a Bruker Avance II 400 MHz spectrometer. Using Agilent 7820A GC system, the GC-MS spectra of products of alcohol oxidation were recorded. Electronic spectra (300–600 nm) were recorded on a Shimadzu UV-vis 1700 spectrophotometer.

Synthesis of ligand

The salophen ligand, N,N'-bis(salicylidene)-1,2-phenylenediamine (**a**) was synthesized by the following established strategy reported in literature⁴³⁻⁴⁴. Anal. CHN analysis % calc. C₂₀H₁₆N₂O₂: C, 75.90 (75.93); H, 5.05 (5.09); N, 8.82 (8.85); MS-ESI (positive, CHCl₃): *m/z*: 317[M+H]⁺, 339[M+Na]⁺; Selected IR frequencies (cm⁻¹, KBr): 1614 (ν_{C=N}: imine), 3400 (ν_{O-H}), 1151 (ν_{C-O}); ¹H NMR (400 MHz, CDCl₃) δ(ppm): 13.10 (s, 2H, OH), 8.62 (s, 2H, CH=N), 7.38–6.90 (m, 12H, Ph); ¹³C NMR (100.62 MHz, CDCl₃) δ (ppm): 163.68 (CH=N), 117.56–161.31 (Ph).

Synthesis of metal complex [Rh(η⁴-L)Cl] (**1a**)

A solution of ligand **a** (0.300 g, 0.94 mmol) in CH₂Cl₂ (5 mL) was added to a solution of RhCl₃.3H₂O (0.250 g, 0.94 mmol) in distilled ethanol

(5 mL) in a 50 mL round bottom flask with continuous stirring (Scheme 1). After refluxing the reaction mixture for 4 h, the compound was washed with hexane, recrystallized from CH₂Cl₂ and finally the complex **1a** was obtained as a brown solid. Yield: 86% Anal. CHN analysis % calc. C₂₀H₁₄N₂O₂ClRh: C, 53.04 (53.11); H, 3.12 (3.10); N, 6.19 (6.12); MS-ESI (positive, DMSO): *m/z*: 415[M-Cl-2H]⁺, 239[M-Rh-Cl-Ph]⁺, 317[M-Rh-Cl+3H]⁺, 211[M-Rh-Cl-PhN₂+H]⁺; Selected IR frequencies (cm⁻¹, KBr): 1631 (ν_{C=N}: imine), 320 (ν_{Rh-Cl}), 1154 (ν_{C-O}); ¹H NMR (400 MHz, DMSO-*d*₆) δ (ppm): 8.77 (s, 2H, CH=N), 8.12–6.94 (m, 12H, Ph); ¹³C NMR (100.62 MHz, DMSO) δ (ppm): 167 (CH=N), 117.20–160.67 (Ph); UV-vis (DMSO) λ_{max} (nm): 320, 340, 458.

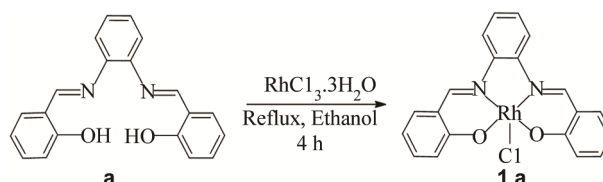
General procedure for the catalytic oxidation of alcohols

A 50 mL round bottom flask was impregnated with alcohol (1 mmol), catalyst **1a** (0.1 mol%), water (10 mL and H₂O₂ 30% (5 mmol)). After refluxing the reaction mixture at 70 °C for the required time, TLC was utilized for monitoring the advancement of the reaction. After the completion of reaction, the mixture was extracted with diethyl ether (3×20 mL) and GC-MS study was carried out.

Results and Discussion

Characterization of complex **1a**

In the FT-IR spectrum, the ν_{C=N} stretching vibration of the free ligand at 1614 cm⁻¹ significantly shifted to higher frequency 1631 cm⁻¹ after complexation, specifying the coordination of imine nitrogen with Rh. Furthermore, the ν_{O-H} stretching band of the free ligand noticed at 3400 cm⁻¹ perished upon complexation, affirming the deprotonation of phenolic moiety and its coordination to Rh. The complex exhibited two new bands at 461 cm⁻¹ and 666 cm⁻¹ which are attributed to ν_{Rh-O} and ν_{Rh-N} stretching bands respectively. The fact has been additionally asserted by the disappearance of phenolic proton signal in the ¹H NMR of **1a** (Supplementary Data, Fig. S1) which appears at δ 13.10 ppm in the free ligand (Supplementary Data, Fig. S2). Upon coordination, a



Synthesis of Rh(III) complex **1a** with Salophen ligand **a**
Scheme 1

marginal downfield shift of imine proton signal occurs from δ 8.62 ppm to δ 8.77 ppm. A similar kind of downfield shift was also noticed for the corresponding carbon in ^{13}C NMR spectrum (Supplementary Data, Fig. S3) of complex which further corroborates the fact that imine nitrogen is involved in coordination with rhodium. The far-IR spectrum of **1a** showed $\nu_{\text{Rh-Cl}}$ band at 320 cm^{-1} . Furthermore, no appearance of curdy white precipitate in AgNO_3 test for **1a** indicates the absence of free Cl^- ion, which designates the coordination of Cl^- to Rh centre. The ESI-mass spectrum of **1a** (Supplementary Data, Fig. S4) shows adequately intense peaks at m/z 415 corresponding to $[\text{M-Cl-2H}]^+$ ion. However, no molecular ion peak was identified. The electronic spectrum of the complex **1a** in DMSO displayed two high intensity peaks at 320 and 340 nm (Supplementary Data, Fig. S5) which are attributed to $\pi \rightarrow \pi^*$ and $n \rightarrow \pi^*$ transition respectively in the ligand moiety. These peaks are transferred to lower energy (red shift) compared to free ligand⁴⁵ which revealed the coordination of the ligand to metal center. The complex also manifested low intensity broad band at 458 nm which may be assigned to $d-d$ transition.

DFT study of complex **1a**

The complex **1a** was fully optimized using double numerical plus polarization (DNP) basis set implemented in DMol3 program package⁴⁶. In order to validate the stability of the complex **1a**, we accomplished vibrational frequency calculations at the optimized structure with the same level of theory. DFT calculations were carried out under generalized gradient approximation (GGA) with B3LYP exchange correlation functional which assimilates exchange functional of Becke's with the gradient corrected

functional of Lee-Yang-Parr. DNP basis set was selected for geometry optimization. DNP basis set is analogous to Gaussian split-valence 6-31G** basis set. Relativistic computations are very significant for heavy metal atoms. Hence, all electron relativistic correction to valence orbitals via a local pseudo potential were accomplished for direct inversion in a subspace method (DIIS) without symmetry constrains. In this study, self consistent field (SCF) procedures were adopted with a convergence criterion of energy 1×10^{-5} Ha, maximum force gradient 2×10^{-3} Ha \AA^{-1} and displacement convergence 5×10^{-3} \AA on the total energy, 10^{-6} a.u. on electron density are the boundary conditions applied.

Initially, structure of ligand **a** and its Rh complex **1a** were fabricated from the existing experimental data in DFT calculations and were fully optimized using B3LYP functional and DNP basis sets as implemented in the program DMol3. The DFT optimized geometries of ligand **a** and complex **1a** are manifested in Fig. 1. In the vibrational frequency calculations, no fictional frequency is noticed for **1a** which recommends that the optimized complex is remarkably stable which shows local minimum in the potential energy surface. All structural variables such as bond distance and bond angles are indicated in Table 1. From the optimized structure, it is observed that the complex **1a** has a distorted pyramidal shape. HOMO-LUMO gap ($\Delta E = E_{\text{LUMO}} - E_{\text{HOMO}}$) and hardness ($\Delta E/2$) values are disclosed in Table 2. It is noted from Table 2 that the complex **1a** is immensely stable as it has high ΔE and hardness value. The HOMO and LUMO of complex **1a** are shown in Fig. 2. The calculated values of Rh-N bond length (2.06 \AA), N-Rh-N bond angle (79.5°) and N-Rh-O bond angle (91.6°) are nearly the same with corresponding

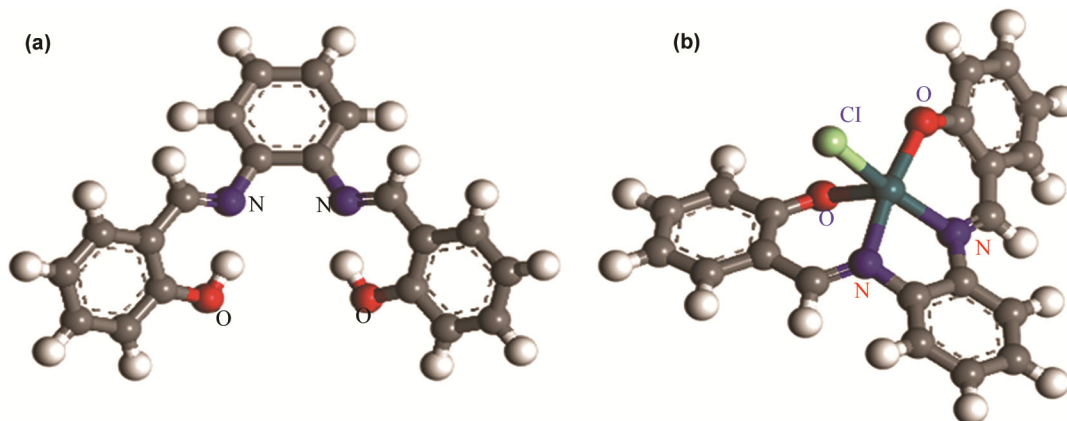
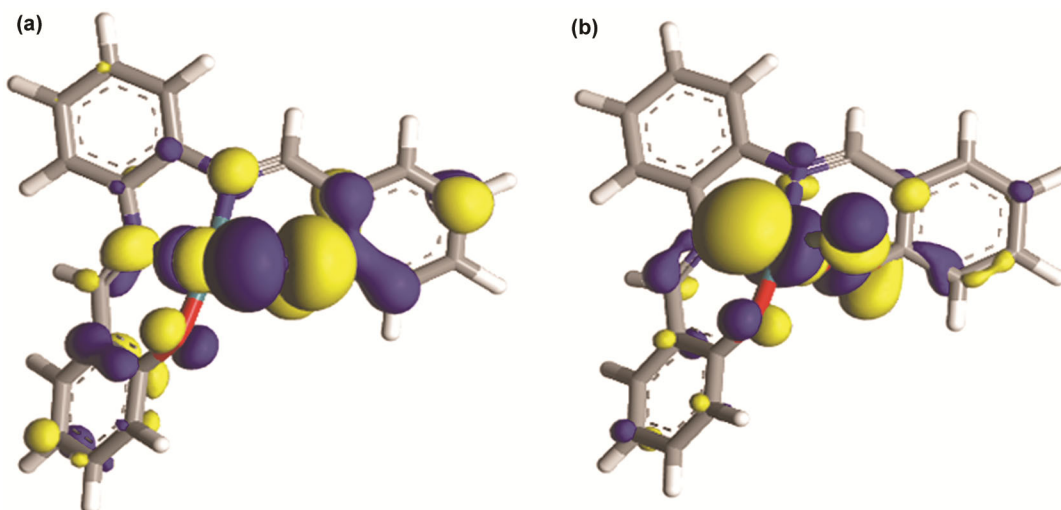


Fig. 1 — DFT optimized geometries of (a) ligand **a** and (b) complex **1a**.

Fig. 2 — (a) HOMO and (b) LUMO of complex **1a**.Table 1 — Selected average bond lengths (Å) and bond angles (°) for Rh complex **1a** evaluated at B3LYP level

Bond	Length (Å)	Bond	Angle (°)
Rh-Cl	2.37	N-Rh-N	79.5
Rh-O	2.03	O-Rh-O	114.5
Rh-N	2.06	N-Rh-Cl	163.7
C=N	1.31	N-Rh-O	91.6
C-O	1.30	O-Rh-Cl	90.5
C=C	1.43		
C-H	1.094		

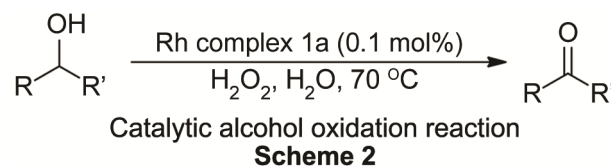
Table 2 — Selected reactivity parameters of ligand **a** and complex **1a** derived at B3LYP level

Compounds	LUMO (eV)	HOMO (eV)	ΔE (eV)	Hardness (eV)
Ligand a	-2.56	-5.06	2.50	1.25
Complex 1a	-3.64	-4.81	1.17	0.58

Zn-salophen complex for which single crystal X-ray structure is reported in literature (Rh-N bond length: 2.06 Å, N-Rh-N bond angle: 79.9° and N-Rh-O bond angle: 89.7°)⁴⁷.

Catalytic activity

To determine optimized reaction condition, the metal complex **1a** was explored as an alcohol oxidation catalyst by considering benzyl alcohol as the representative substrate (Scheme 2). Different protic and non-protic solvents and oxidants like H₂O₂, air and O₂ were utilized. At first, the reactions were carried out using 0.1 mol% catalyst **1a** with H₂O₂ as oxidant in different solvents without the addition of any auxiliary base. With change of solvents, a remarkable variation of yields was observed (Table 3)

Table 3 — Optimization of solvent for oxidation of benzyl alcohol using H₂O₂

Entry	Solvent	Time (h)	Yield (%) ^a
1	CH ₃ CN	3	38
2	CH ₃ CN:H ₂ O	2	62
3	H ₂ O	2	91
4	ⁱ PrOH	3	32
5	ⁿ BuOH	3	22
6	CH ₂ Cl ₂	3	24

reaction conditions: benzyl alcohol (1 mmol), H₂O₂ (5 mmol, 30%), solvent (10 mL). ^aGC yields.

and water manifested as the best solvent with 91% yield at reaction time of 2 h. As our catalyst is a homogeneous one, it can easily interact with the substrate molecule at the interface facilitating oxidation reaction and such type of system has been reported in literature. Moreover, effectiveness of different oxidants was explored using water as solvent (Table 4). Initially, the oxidation reaction was conducted under aerobic condition at room temperature by bubbling air through an aqueous solution of benzyl alcohol in the presence of 0.2 mol% catalyst. After 24 h of reaction time, 30% conversion was monitored by GC (Table 4; entry 1). When the same reaction was carried out by bubbling molecular O₂, minimal improvement in conversion was noted. Nevertheless, on using H₂O₂ much higher

conversion was noticed at room temperature. Remarkable increase in yield was feasible on increasing the reaction temperature to 70 °C. However, under the identical condition, neat RhCl₃·3H₂O as catalyst exhibited only 15% conversion (Table 4; entry 7). This indicates that the presence of ligand in the complex substantially influences the catalytic efficiency by increasing

electron density on metal centre. It may be important to mention here that while the reactions are performed with excess H₂O₂ at elevated temperature, there is a possibility of formation of free radicals (●OH or ●OOH) which may facilitate the oxidation reaction. To investigate this, we have performed a controlled experiment with benzyl alcohol without adding the catalyst, but no conversion was observed which ruled out the involvement of free radicals in the oxidation process (Table 4; entry 6). Transition metal catalyzed oxidation of alcohols is a well-established method and its mechanism is also well documented in literatures¹⁶. Usually, the process involves the formation of a metal oxo intermediate followed by oxygen transfer. In our case also, we expect a similar mechanistic pathway for the alcohol oxidation reaction

To assess the scope and limitations of the catalyst **1a**, reactions of a broad range of electronically diverse primary and secondary alcohols were investigated under optimized conditions and the results are outlined in Table 5 (GC-MS spectra are given as supplementary Data, Fig. S6-S21). The catalyst displayed excellent activity for the selective

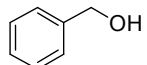
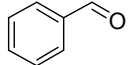
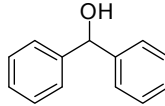
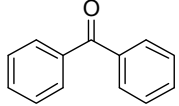
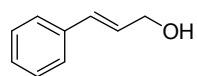
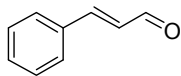
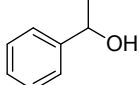
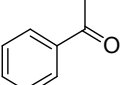
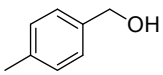
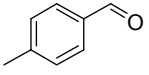
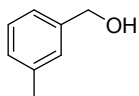
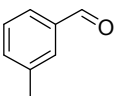
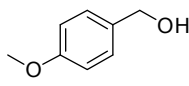
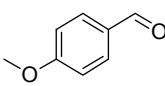
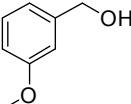
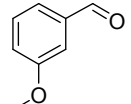
Table 4 — Optimization of reaction condition for oxidation^a of benzyl alcohol using various oxidants

Entry	Catalyst	Oxidant	Temp (°C)	Time (h)	Rh (mol %)	Yield ^b (%)
1	1a	Air	rt	24	0.2	30
2	1a	O ₂	rt	24	0.2	35
3	1a	H ₂ O ₂	rt	24	0.2	61
4	1a	H ₂ O ₂	60	3	0.2	78
5	1a	H ₂ O ₂	70	2	0.1	91
6	-	H ₂ O ₂	70	2	-	-
7	RhCl ₃ ·3H ₂ O	H ₂ O ₂	70	2	0.2	15

^areaction conditions: benzyl alcohol (1 mmol), H₂O₂ (5 mmol, 30%)/air/O₂ (1 atm), water (10 mL).

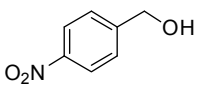
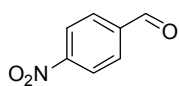
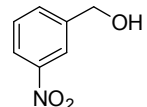
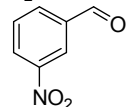
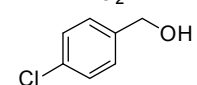
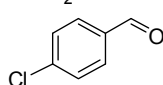
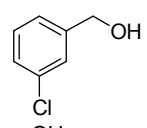
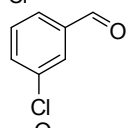
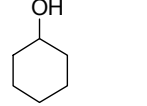
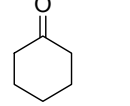
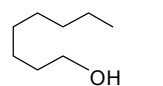
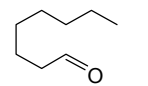
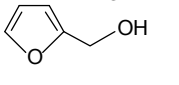
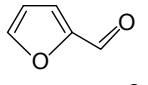
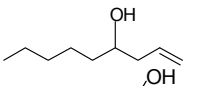
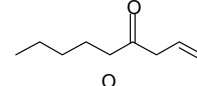
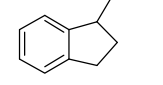
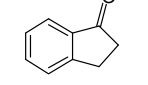
^bGC yields.

Table 5 — Oxidation reactions of various alcohols in aqueous media catalysed by **1a** using H₂O₂

Entry	Alcohols	Products	Time (h)	Yield (%) ^a
1			2	91
2			2	78
3			3	51
4			3	72
5			2	98
6			2	88
7			3	84
8			3	56

(Contd.)

Table 5 — Oxidation reactions of various alcohols in aqueous media catalysed by **1a** using H₂O₂ (Contd.)

Entry	Alcohols	Products	Time (h)	Yield (%) ^a
9			3	65
10			3	38
11			3	78
12			3	52
13			3	62
14			3	28
15			3	57
16			3	34
17			2	99

^aGC yields.

oxidation of various substituted benzyl alcohols, although a wide variation in yields was observed. Benzyl alcohols possessing electron donating substituents at *para* position (e.g., -Me, -OMe,) (entries 5 and 7) gave the desired product in good yields while those bearing electron withdrawing groups such as *p*-NO₂, *p*-Cl (entries 9 and 11) resulted in comparatively lower conversions. It is fascinating to note here that the position of substituents has significant effect on the catalytic performances. For example, the oxidation of *m*-nitrobenzyl alcohol gave only 38% product, while under identical experimental conditions *p*-nitrobenzyl alcohol gave 65% aldehyde (entry 10 versus entry 9). The results evidently demonstrate that under the optimized reaction condition, virtually quantitative yields of carbonyl compounds have been obtained with a range of secondary alcohols such as benzhydrol, 1-phenylethanol and cyclohexanol, whereas 1-indanol gave outstanding yield in just 2 h. Furthermore, allylic alcohols such as cinnamyl alcohol and heterocyclic alcohols like furfuryl alcohol, which are considered as

difficult substrates for oxidation reaction, could be oxidized with good yields.

Conclusions

A new rhodium(III) complex **1a** comprising salophen ligand was synthesized and characterized by employing FT-IR, UV-vis, ESI-MS, ¹H and ¹³C NMR spectroscopy. The Rh centre of the complex is coordinated to the two N and O donor sites of the salophen ligand together with a coordinatively bonded Cl⁻. The complex was investigated as a catalyst for selective oxidation of alcohol using extensive variety of sterically and electronically diversified substrates and unveiled good to excellent results using H₂O₂ as oxidant in aqueous medium under base-free conditions.

Supplementary Data

Supplementary Data associated with this article are available in the electronic form at [http://www.niscair.res.in/jinfo/ijca/IJCA_58A\(01\)29-35_SupplData.pdf](http://www.niscair.res.in/jinfo/ijca/IJCA_58A(01)29-35_SupplData.pdf).

Acknowledgement

The DST, New Delhi, India is gratefully acknowledged for financial support (Project No: EMR/2015/000021). The UGC, New Delhi, India has also been acknowledged for the SAP-DRS-I grant to the Department of Chemistry and for awarding a minor project to BB (Project No: F. 5-191/2015-16/MRP/NERO/357). The SAIF, Punjab University, IISC Bangalore and IIT Madras, India are gratefully acknowledged for various analytical services.

References

- Tojo G & Fernandez M, *Oxidation of Alcohols to Aldehydes and Ketones: A Guide to Current Common Practice*, (Springer, Boston, MA) 2006.
- Albonetti S, Mazzoni R & Cavani F, *Transition Metal Catalysis in Aerobic Alcohol Oxidation*, (RSC, Cambridge, UK), 2014, p. 1.
- Sheldon R A & Kochi J K, *Metal-Catalyzed Oxidations of Organic Compounds*, 1st edn, (Academic Press, New York) 1981.
- Parmeggiani C & Cardona F, *Green Chem*, 14 (2012) 547.
- Sheldon R A, *Catal Today*, 247 (2015) 4.
- Kopylovich M N, Ribeiro A P C, Alegria E C B A, Martins N M R, Martins L M D R S & Pombeiro A J L, *Adv Organomet Chem*, 63 (2015) 91.
- Assady E, Yadollahi B, Farsani M R & Moghadam M, *Appl Organomet Chem*, 29 (2015) 561.
- Tandon P K, Gayatri, Sahgal S, Srivastava M & Singh S B, *Appl Organomet Chem*, 21 (2007) 135.
- Wu J, Liu Y, Ma X, Liu P, Gu C & Dai B, *Appl Organometal Chem*, 30 (2016) 577.
- Kani I & Bolat S, *Appl Organomet Chem*, 30 (2016) 713.
- Lou J-D & Xu Z-N, *Tetrahedron Lett*, 43 (2002) 6095.
- Corey E J & Suggs J W, *Tetrahedron Lett*, 16 (1975) 2647.
- Fatiadi A J, *Synthesis*, 1987 (1987) 85.
- Sahu D, Banik B, Borah M & Das P, *Lett Org Chem*, 11 (2014) 671.
- Srour H, Maux P L, Chevance S & Simonneaux G, *Coord Chem Rev*, 257 (2013) 3030.
- Landaeta V R & Rodríguez Lugo R E, *Inorg Chim Acta*, 431 (2015) 21.
- Marui K, Higashiura Y, Kodama S, Hashidate S, Nomoto A, Yano S, Ueshima M & Ogawa A, *Tetrahedron*, 70 (2014) 2431.
- Bailie D S, Clendenning G M A, McNamee L & Muldoon M J, *Chem Comm*, 46 (2010) 7238.
- Jiang J A, Du J L, Wang Z G, Zhang Z N, Xu X, Zheng G L & Ji Y F, *Tetrahedron Lett*, 55 (2014) 1677.
- Zhang G, Li L, Yang C, Liu E, Golen J A & Rheingold A L, *Inorg Chem Comm*, 51 (2015) 13.
- Yan Y, Tong X, Wang K & Bai X, *Catal Comm*, 43 (2014) 112.
- Rezaeivala M & Keypour H, *Coord Chem Rev*, 280 (2014) 203.
- Singh Y P, Patel R N & Singh Y, *Ind J Chem*, 57A (2018) 44.
- Cozzi P G, *Chem Soc Rev*, 33 (2004) 410.
- Zoubi W A & Ko Y G, *Appl Organometal Chem*, 31 (2016) 1.
- Zoubi W A & Ko Y G, *J Organomet Chem*, 822 (2016) 173.
- Li X, Ma D, Cao B & Lu Y, *New J Chem*, 41 (2017) 11619.
- Bhattacharjee A, Halder S, Ghosh K, Rizzoli C & Roy P, *New J Chem*, 41 (2017) 5696.
- Kadwa E, Friedrich H B & Bala M D, *Inorg Chim Acta*, 463 (2017) 112.
- Biswas S, Roy P, Sarkar D & Mondal T K, *Ind J Chem*, 55A (2016) 929.
- Gupta K C & Sutar A K, *Coord Chem Rev*, 252 (2008) 1420.
- Voronova K, Purgel M, Udvardy A, Bényei A C, Kathó A & Joó F, *Organometallics*, 32 (2013) 4391.
- Himeda Y, Onozawa-Komatsuzaki N, Sugihara H, Arakawa H & Kasuga K, *J Mol Catal A: Chem*, 195 (2003) 95.
- Grivani G, Khalaji A D, Tahmasebi V, Gotoh K & Ishida H, *Polyhedron*, 31 (2012) 265.
- Egekenze R, Gultneh Y & Butcher R, *Polyhedron*, 144 (2018) 198.
- Das P & Linert W, *Coord Chem Rev*, 311 (2016) 1.
- Ansari R M & Bhat B R, *J Chem Sci*, 129 (2017) 1483.
- Sedighipour M, Kianfar A H, Mohammadnezhad G, Görls H & Plass W, *Inorg Chim Acta*, 476 (2018) 20.
- Banik B, Tairai A, Shanaz N & Das P, *Tetrahedron Lett*, 53 (2012) 5627.
- Shanaz N, Banik B & Das P, *Tetrahedron Lett*, 54 (2013) 2886.
- Shanaz N, Puzari A, Paul B & Das P, *Catal Commun*, 86 (2016) 55.
- Banik B, Tairai A, Bhattacharyya P K & Das P, *Appl Organometal Chem*, 30 (2016) 519.
- Amirnasr M, Schenk K J, Gorji A & Vafazadeh R, *Polyhedron*, 20 (2001) 695.
- Singh T S, Paul P C & Pramanik H A R, *Spectrochim Acta Part A*, 121 (2014) 520.
- Zhou L, Cai P, Feng Y, Cheng J, Xiang H, Liu J, Wu D & Zhou X, *Analyt Chim Acta*, 735 (2012) 96.
- Delly B, *J Chem Phys*, 92 (1990) 508.
- Hosseinnejad T, Dehghanpour S & Hosseinjani A, *Comp Theor Chem* 1004 (2013) 31.